

## Tailoring the exchange bias via shape anisotropy in ferromagnetic/antiferromagnetic exchange-coupled systems

A. Hoffmann,\* M. Grimsditch, and J. E. Pearson

*Materials Science Division, Argonne National Laboratory, Argonne, Illinois 60439, USA*

J. Nogués

*Institució Catalana de Recerca i Estudis Avançats and Departament de Física, Universitat Autònoma de Barcelona, 08193 Bellaterra, Spain*

W. A. A. Macedo

*Laboratório de Física Aplicada, Centro de Desenvolvimento da Tecnologia Nuclear, 30123-970 Belo Horizonte, Minas Gerais, Brazil*

Ivan K. Schuller

*Department of Physics, University of California–San Diego, La Jolla, California 92093-0319, USA*

(Received 8 May 2003; published 26 June 2003)

The magnetic behavior of Fe lines on top of a continuous  $\text{FeF}_2$  antiferromagnetic layer was investigated as a function of the orientation of the lines with respect to the applied magnetic field and a unidirectional anisotropy established by field cooling. The orientational dependence of the asymmetric loop shift, called exchange bias, shows that the competition between shape and unidirectional anisotropies modifies the exchange bias and the coercivity. Remarkably, in certain cases, exchange bias can be observed even when the applied field is perpendicular to the unidirectional anisotropy. Numerical simulations with a coherent rotation model illustrate a rich phase diagram, which originates from the noncollinearity of the involved anisotropies. Using this phase diagram, exchange bias and coercivity can be predictably tailored. In particular, different preferred magnetization directions can be designed in separately patterned structures of the same sample with identical preparation and magnetic history.

DOI: 10.1103/PhysRevB.67.220406

PACS number(s): 75.75.+a, 75.60.Ej, 75.70.Cn

Although the role of shape anisotropy in homogeneous magnetic materials has been well understood for a long time,<sup>1–3</sup> we show here that adding shape anisotropy to magnetic heterostructures can give rise to an unexpected behavior due to a competition between shape anisotropy and internal interactions of the heterostructure. Examples of heterostructures, which received much attention lately, are ferromagnetic/antiferromagnetic exchange-coupled systems. The coupling between an antiferromagnet and a ferromagnet can give rise to an induced *unidirectional* anisotropy in the ferromagnet, which is referred to as exchange bias. The main characteristic of this induced anisotropy is a shift of the hysteresis loop of the ferromagnet along the field axis.<sup>4</sup> This unidirectional anisotropy stems presumably from the way the antiferromagnet orders in the proximity of a ferromagnet, but a detailed understanding is still missing.<sup>5</sup> Regardless of the missing microscopic understanding, exchange bias has become important for many magnetoelectronic applications, because it pins the magnetization orientation of one ferromagnetic layer, which then serves as the reference layer in a variety of device structures, such as spin valves and magnetic memory elements.<sup>6</sup>

For applications, it is often necessary to pattern the heterostructures into a confined geometry. Thus the question of how patterning influences the magnetic behavior arises naturally. Up to now, studies of exchange-biased antiferromagnetic/ferromagnetic wires have been restricted to cases with shape anisotropy either parallel or perpendicular to the applied magnetic field.<sup>7,8</sup> These studies showed a modified

exchange bias similar to nanostructured networks of exchange-bias systems.<sup>9,10</sup> However, there has been no systematic study of the role of the shape anisotropy orientation and no quantitative understanding of these effects has yet been obtained.

In this work, we studied the exchange bias of Fe lines on an antiferromagnetic  $\text{FeF}_2$  film as a function of line orientation with respect to cooling and applied magnetic fields, but fixed with respect to the  $\text{FeF}_2$  crystalline orientations. The main result is that competition and noncollinearity between unidirectional exchange coupling and shape anisotropy can give rise to an unexpected magnetic behavior. This opens up a straightforward pathway to tailor both the *magnitude* and *direction* of exchange bias, which can be applied to any exchange-bias system. We compare the experimental results to numerical simulations obtained from a coherent rotation model. The simulations give rise to a surprisingly rich variety of hysteretic behavior. The magnetic behavior depends strongly on the ratio and relative orientation between shape and uniaxial anisotropies. In particular, when the ratio is less than 1, large exchange bias is observed even with magnetic fields applied perpendicular to the unidirectional anisotropy. This permits the introduction of several different preferred magnetization directions in separately patterned structures, independent from material specific parameters, even if they have identical magnetic history.

Using *e*-beam lithography and ion milling, we defined 300-nm-wide polycrystalline Fe lines on top of a continuous quasiepitaxial (110)  $\text{FeF}_2$  film grown on  $\text{MgO}(100)$ . The

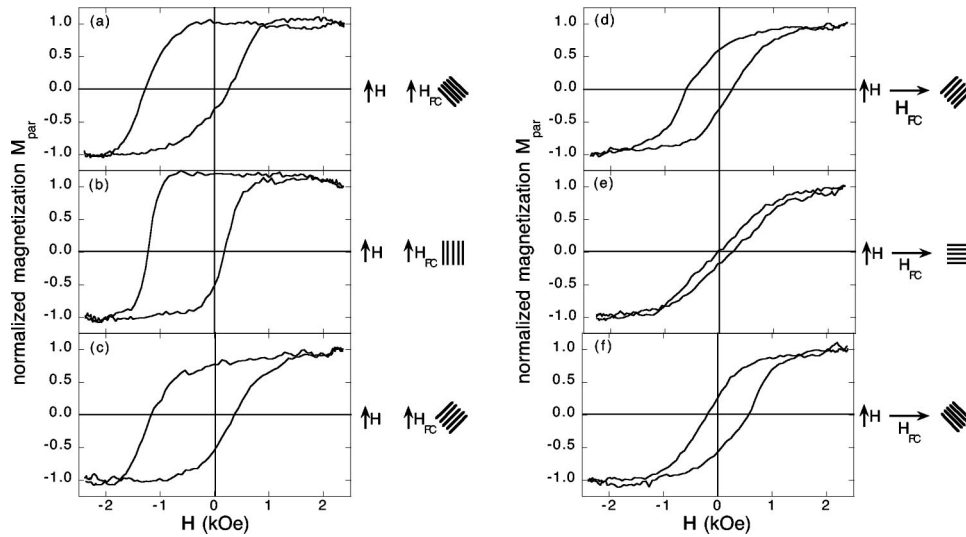


FIG. 1. Hysteresis loops measured with MOKE at 35 K for three patterns with the lines  $-45^\circ$  (a,d),  $0^\circ$  (b,e), and  $+45^\circ$  (c,f) oriented with respect to the cooling field and the applied field during the hysteresis loop measurements. The applied magnetic field is parallel to the cooling field for (a)–(c), while it is perpendicular for (d)–(f). The directions of the applied field and cooling field with respect to the lines are indicated to the right of each plot. Note that  $H_{FC}$  is always applied along  $[010]$  MgO (corresponding to either  $[1\bar{1}2]$  or  $[\bar{1}12]$  of the two  $\text{FeF}_2$  twins, respectively).

$\text{FeF}_2$  layer has a twinned in-plane structure, such that  $[001]$   $\text{FeF}_2$  is along either  $[011]$  or  $[0\bar{1}1]$  of the MgO substrate.<sup>11</sup> The  $\text{FeF}_2$  and Fe are 90 and 10 nm thick, respectively. The Fe lines have a periodicity of 500 nm and cover several  $100 \times 100\text{-}\mu\text{m}^2$  areas, each with a different direction with respect to the MgO  $[010]$  direction. Since all the patterns are on one single chip, it is assured that the local exchange interaction between the Fe lines and  $\text{FeF}_2$  film and the magnetic history (i.e., magnitude and direction of the cooling field) are identical for all patterns.

The magnetic hysteresis loops of the line patterns were measured with magneto-optic Kerr effect (MOKE),<sup>12</sup> using an optical cryostat. The transverse MOKE geometry<sup>12</sup> is used under  $\approx 45^\circ$  incidence, which allows us to measure the magnetization component  $M_{par}$  parallel to the applied field. The laser beam is focused down to  $50\ \mu\text{m}$  diameter, which enables us to address each of the Fe-line patterns individually. Magnetic hysteresis loops measured at room temperature for the patterned Fe lines along various directions are consistent with a uniaxial shape anisotropy  $K_u = 150\ \text{Oe}$ .

For measurements in the exchange-biased state, the sample is cooled from room temperature to 35 K in an applied field of 1.5 kOe. It should be noted that depending on the crystalline orientation of the antiferromagnet, the unidirectional exchange-coupling anisotropy is not necessarily along the cooling field direction.<sup>13</sup> However, here we always apply the cooling field along MgO  $[010]$  (corresponding to either  $[1\bar{1}2]$  or  $[\bar{1}12]$  of the two  $\text{FeF}_2$  twins, respectively), which guarantees that in our case the cooling field direction and the direction of unidirectional anisotropy are identical.<sup>13</sup> Figures 1(a)–1(c) show magnetic hysteresis loops after field cooling for three patterns with the lines oriented at  $-45^\circ$ ,  $0^\circ$ , and  $+45^\circ$  relative to the cooling and the applied field. The resulting exchange bias is similar ( $H_E \approx 475\ \text{Oe}$ ) for all three patterns and only the shape of the hysteresis loop is somewhat changed by the different shape anisotropies. Furthermore, as expected, the hysteresis loops for the patterns rotated  $+45^\circ$  or  $-45^\circ$  [see Figs. 1(a) and 1(c)] are essentially identical.

As shown in Figs. 1(d)–1(f), the situation is completely

different as soon as the patterns are rotated  $90^\circ$  clockwise after field cooling. The unidirectional anisotropy is now perpendicular to the applied magnetic field and therefore one would naively not expect to observe any exchange bias. Indeed, for the pattern where the cooling field direction is parallel to the lines and thus along the direction of the uniaxial shape anisotropy, the exchange bias is negligible compared to the other cases [see Fig. 1(e)]. On the other hand, for the lines at  $45^\circ$  to both the applied and the cooling fields, there is an exchange bias [see Figs. 1(d) and 1(f)]. However, note that the sign of the exchange bias is opposite for the two orientations, even though the magnetic history is exactly the same.

It is instructive to compare these experimental results with numerical simulations based on a coherent rotation model (Stoner-Wohlfarth type<sup>2</sup>) similar to earlier works.<sup>14,15</sup> If we assume a homogeneous magnetization in the Fe lines, then the free energy  $f$  can be written as

$$f = -HM_s \cos \theta - K_E \cos(\theta - \theta_E) - K_u \cos^2(\theta - \theta_u), \quad (1)$$

where  $H$  is the applied field,  $M_s$  is the saturation magnetization,  $\theta$  is the angle of the magnetization with the applied field,  $K_E$  and  $K_u$  are the *unidirectional* exchange coupling and the *uniaxial* shape anisotropy, and  $\theta_E$  and  $\theta_u$  are the angles between the applied field and these two anisotropy axes, respectively. Hysteresis loops are determined numerically via energy minimization of Eq. (1). Results are shown in Fig. 2 for different ratios of  $K_u/K_E$  and fixed values of  $\theta_E = 90^\circ$  and  $\theta_u = 45^\circ$ , corresponding to the case in Fig. 1(d). As one can see, a range of hysteretic behavior can be observed depending on the ratio  $K_u/K_E$ .

The exchange bias  $H_E$  and the coercivity  $H_c$  values extracted from these simulated loops are plotted as a function of  $K_u/K_E$  in Fig. 3. One can distinguish three types of behavior. For vanishing  $K_u$ ,  $H_E$  also vanishes and the magnetization simply rotates reversibly from one direction to the opposite, whereby at remanence the magnetization always points along the unidirectional anisotropy  $K_E$  [see Fig. 2(a)]. With increasing  $K_u$  the magnetization still rotates reversibly, albeit asymmetrically [see Fig. 2(b)]. This gives rise to an

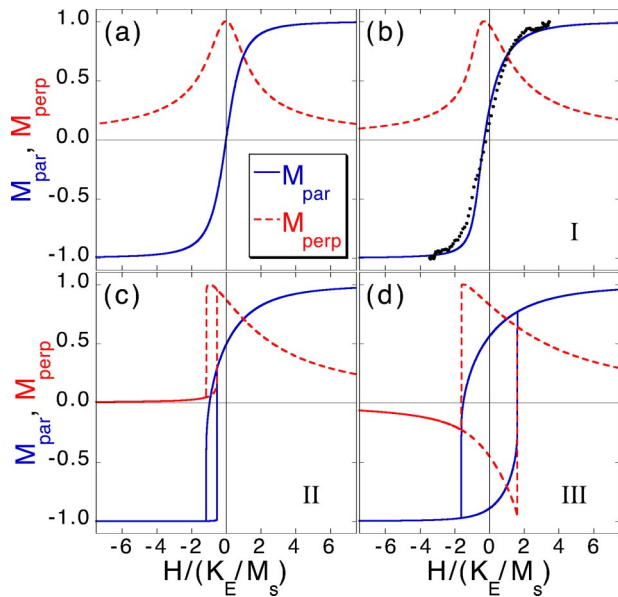


FIG. 2. (Color online) Hysteresis loops from the coherent rotation model with  $\theta_E$  and  $\theta_u$  fixed to  $90^\circ$  and  $45^\circ$ , respectively. Shown are the longitudinal (solid line) and transverse (dashed line) magnetizations  $M_{par}$  and  $M_{perp}$  normalized by the saturation magnetization. The curves are for  $K_u/K_E$  ratios of 0 (a), 0.3 (b), 0.95 (c), and 1.5 (d). The solid symbols in (b) indicate the average of the two hysteresis branches from Fig. 1(d).

$H_E$  which increases linearly with  $K_u$  [see region I in Fig. 3]. When  $K_u/K_E$  reaches 0.85, the hysteresis loop shows irreversible behavior [see Fig. 2(c)]. Notice that the exact value at which the irreversible behavior becomes important depends on the angle between the uniaxial and the unidirectional anisotropy. For  $K_u/K_E$  larger than 0.85,  $H_c$  increases and  $H_E$  decreases [see region II in Fig. 3] until they both become close to  $K_E/2M_s$  near  $K_u/K_E = 1$ . For  $K_u/K_E < 1$ , the perpendicular component of the magnetization always points along the direction of the unidirectional anisotropy during the magnetization reversal. The situation changes

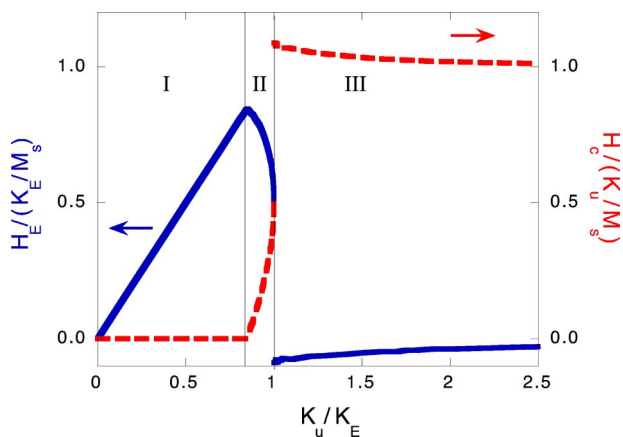


FIG. 3. (Color online) Calculated  $H_E$  (solid line) and  $H_c$  (dashed line) normalized by  $K_E/M_s$  and  $K_u/M_s$ , respectively, as a function of  $K_u/K_E$  at fixed  $\theta_E = 90^\circ$  and  $\theta_u = 45^\circ$ . The regions of different hysteresis behavior are indicated by I, II, and III.

completely at  $K_u = K_E$ . There is a first-order transition in the hysteretic behavior, such that the magnetization reverses in opposite directions during the ascending and descending branches of the hysteresis loop [see Fig. 2(d)]. At the same time  $H_c$  increases by more than a factor of 2, such that  $H_c > K_u$ , and  $H_E$  changes sign and is significantly reduced in magnitude. Upon further increasing  $K_u$ ,  $H_E$  vanishes, and  $H_c$  becomes equal to  $K_u$  [see region III in Fig. 3] as is expected for a coherent rotation model without additional unidirectional anisotropy.<sup>2</sup>

It is important to realize that the complexity of this magnetic behavior is due to the noncollinearity of the applied field, the unidirectional exchange-coupling anisotropy established by the field cooling, and the shape anisotropy determined by the geometry. For example, if the unidirectional anisotropy is parallel to the applied field, then the exchange bias is independent of the shape anisotropy, namely,  $H_E = K_E/M_s$ , which is exactly the experimental observation [see Figs. 1(a)–1(c)]. It should also be pointed out that the calculated hysteresis loops do not require that the uniaxial anisotropy be due to the shape of the ferromagnet. If the ferromagnet has an intrinsic uniaxial anisotropy (i.e., crystalline<sup>15</sup>), then the same effects should be observable. However, unlike crystalline uniaxial anisotropy, shape anisotropy introduces an extra degree of freedom, since different parts of the same sample can be designed to have different magnitude and direction of shape anisotropy.

We can estimate, which region of Fig. 3 corresponds to the samples we measured. The shape anisotropy of the Fe lines can be calculated from demagnetizing factors if one approximates the wires as general ellipsoids. Using  $M_s = 1740$  emu/cm<sup>3</sup> for Fe and the dimensions of 100  $\mu$ m length, 300 nm width, and 10 nm thickness results in  $K_u/M_s = 353$  Oe.<sup>3</sup> This compares well with the shape anisotropy determined from room-temperature, hard-axis hysteresis loops, which show an anisotropy field  $H_a \approx 300$  Oe, corresponding to  $K_u/M_s \approx 150$  Oe. The unidirectional exchange-coupling anisotropy can be determined directly from measurements with the field applied along the field cooling direction [Figs. 1(a)–1(c)] and is  $K_E/M_s = H_E = 475$  Oe. Thus, the samples correspond to region I in Fig. 3. Therefore the exchange bias should be equal to  $K_u/M_s$ , and in fact the exchange bias in Figs. 1(d) and 1(f) is  $\pm 180$  Oe, corresponding well to  $K_u/M_s = 150$  Oe, determined from the room-temperature hysteresis loops. Of course, one may notice that the simulation in Fig. 2(b) does not show any hysteresis in contrast to the experimental data. This is most likely due to the fact that the model ignores more complicated origins of coercivity in exchange-bias systems, such as irreversible losses in the antiferromagnet.<sup>16</sup> These contributions can be removed from the experimental data by averaging the branches of the two hysteresis loops and the result is shown by the solid symbols in Fig. 2(b) together with the corresponding numerical simulation. The result is remarkable, since without any free parameter, not only the shift of the loop but also the overall shape of the loop are well described.

In the past, various other approaches have been used successfully to modify exchange bias locally, for example, by

ion irradiation.<sup>17</sup> One distinct advantage of the work presented here is that the use of shape anisotropy provides precise control of the magnitude and orientation (i.e., sign) of the exchange bias over a wide range. This means that once the unidirectional exchange-coupling anisotropy is known (i.e., from an unpatterned film), the coherent rotation model can be used to predict *quantitatively* the resulting exchange-bias shifts of the patterned areas.

In conclusion, we have proven that uniaxial shape anisotropy can give rise to exchange bias in situations where one naively would not expect any. Numerical simulations based on a coherent rotation model show that this effect relies on the noncollinearity of the involved anisotropies. The exchange bias is most pronounced when the uniaxial anisotropy is slightly smaller than the unidirectional exchange-bias anisotropy. Furthermore, as a function of the ratio between the uniaxial and the unidirectional anisotropy  $K_u/K_E$ , the numerical simulations provide a phase diagram with three regions of hysteretic behavior and a change of sign for the exchange bias. Future experiments with varying ratios of

$K_u/K_E$  should be able to explore the full range of predicted hysteretic behavior. Furthermore, the directional selectivity of the exchange bias due to shape anisotropy can be used to establish different preferred magnetization directions in separately patterned structures with the same magnetic history. Similarly, one can expect that the competition between shape anisotropy and internal interactions in other types of magnetic heterostructures can give rise to equally rich varieties of magnetic behavior.

We would like to acknowledge technical assistance from J. S. Jiang, W.-T. Lee, M. I. Montero, V. Novosad, and P. Vavassori, as well as stimulating discussions with T. Schultess. We would also like to thank S. D. Bader for a critical reading of the manuscript. W.A.A.M. gratefully acknowledges the hospitality during his stay at UCSD. This work was supported by the U.S. Department of Energy, BES-DMS under Contract No. W-31-109-ENG-38, U.S. AFOSR, CICYT (Grant No. MAT2001-2555), DGR (Grant No. 2001SGR00189), and CNPq (Brazil).

\*Electronic address: hoffmann@anl.gov

<sup>1</sup>J.I. Martín, J. Nogués, K. Liu, J.L. Vicent, and I.K. Schuller, *J. Magn. Magn. Mater.* **256**, 449 (2003).

<sup>2</sup>E.C. Stoner and E.P. Wohlfarth, *Philos. Trans. R. Soc. London, Ser. A* **240**, 74 (1948).

<sup>3</sup>J.A. Osborn, *Phys. Rev.* **67**, 351 (1945).

<sup>4</sup>W.H. Meiklejohn and C.P. Bean, *Phys. Rev.* **102**, 1413 (1957).

<sup>5</sup>J. Nogués and I.K. Schuller, *J. Magn. Magn. Mater.* **192**, 203 (1999).

<sup>6</sup>J.C.S. Kools, *IEEE Trans. Magn.* **32**, 3165 (1996).

<sup>7</sup>A. Nemoto, Y. Otani, S.G. Kim, K. Fukamichi, O. Kitakami, and Y. Shimada, *Appl. Phys. Lett.* **74**, 4026 (1999).

<sup>8</sup>M. Fraune, U. Rüdiger, G. Güntherodt, S. Cardoso, and P. Freitas, *Appl. Phys. Lett.* **77**, 3815 (2000).

<sup>9</sup>K. Liu, S.M. Baker, M. Tuominen, T.P. Russell, and I.K. Schuller, *Phys. Rev. B* **63**, 060403(R) (2001).

<sup>10</sup>L. Sun, Y. Ding, C.L. Chien, and P.C. Searson, *Phys. Rev. B* **64**, 184430 (2001).

<sup>11</sup>J. Nogués, T.J. Moran, D. Lederman, I.K. Schuller, and K.V. Rao, *Phys. Rev. B* **59**, 6984 (1999).

<sup>12</sup>S.D. Bader, *J. Magn. Magn. Mater.* **100**, 440 (1991).

<sup>13</sup>H. Shi and D. Lederman, *Phys. Rev. B* **66**, 094426 (2002).

<sup>14</sup>W.H. Meiklejohn and C.P. Bean, *Phys. Rev.* **105**, 904 (1957).

<sup>15</sup>T. Mewes, H. Nembach, M. Rickart, S.O. Demokritov, J. Fassbender, and B. Hillebrands, *Phys. Rev. B* **65**, 224423 (2002).

<sup>16</sup>M.D. Stiles and R.D. McMichael, *Phys. Rev. B* **63**, 064405 (2001).

<sup>17</sup>J. Fassbender *et al.*, *Phys. Status Solidi A* **189**, 439 (2002).